

Design, simulation and fabrication of piezoelectric micro generators for aero acoustic applications

Aliza Aini Md Ralib · Anis Nurashikin Nordin ·
Raihan Othman · Hanim Salleh

Received: 25 June 2010 / Accepted: 7 January 2011 / Published online: 5 February 2011
© Springer-Verlag 2011

Abstract Energy harvesters based on acoustic vibration sources can generate electrical power through piezoelectric transduction. Significant miniaturization of electro mechanical devices using MEMS fabrication technology has encouraged the creation of portable, miniature energy harvesters. A niche application is aero acoustics, where wasted, high dB and high frequency sound generated by aircrafts are transformed into useful energy. Having self-powered, miniature acoustic sensors allows noise detection monitoring systems to be self-sustaining. This paper illustrates an Aluminium doped Zinc Oxide (AZO) cantilever beam on stainless steel substrate with a top copper electrode. Design and finite element modelling of the design was conducted using Coventorware™. The AZO piezoelectric thin film was RF-sputtered on the stainless steel substrate. Characterizations were performed using X-ray diffraction (XRD) and scanning electron microscopy (SEM) to evaluate the piezoelectric qualities and surface morphology, respectively. Experimental measurements

indicate approximately 345.4 mV AC output voltage (open circuit voltage) is produced at vibration frequencies of 30 kHz. This is in accordance with the Coventorware™ simulation results. This measured power level is sufficient to power a miniature wireless acoustic sensor nodes to monitor noise generated by aircrafts.

1 Introduction

Energy harvesters have become significantly popular and crucial due to accelerated increase in demand of self-sustaining devices. Self-powered micro scale energy harvesting devices is a promising solution to replace conventional batteries that have limited lifetime, bulky and contain hazardous chemicals. Several publications covering wide range of energy harvesting applications have been published recently (Paradiso and Starner 2005; Kok et al. 2008; Liu et al. 2008; Choi et al. 2006).

Energy can be scavenged from various environment sources such as solar, wind, light and vibration. Solar energy is frequently used but it is not an attractive source for indoor environments (Kim et al. 2009). Among these methods, mechanical vibration and acoustic sources provide the most potential solution for energy harvesting. There are three transduction mechanisms for vibration based energy harvesting, piezoelectric, electromagnetic and electrostatic transduction (Roundy et al. 2005). Of the three mechanisms, piezoelectric transducers have been reported to produce the highest power output for a given size (Roundy et al. 2005). A piezoelectric energy micro-generator typically harvests mechanical energy or vibrations and converts it to electrical energy through piezoelectric effect. The micro-cantilever structure is typically used due to its high power output and compatibility with

A. A. Md Ralib (✉) · A. N. Nordin
Department of Electrical and Computer Engineering,
International Islamic University, Kuala Lumpur,
Malaysia
e-mail: aliza.aini@gmail.com

A. N. Nordin
e-mail: anisnn@iiu.edu.my

R. Othman
Department of Science in Engineering, International Islamic
University, Kuala Lumpur, Malaysia
e-mail: raihan@iiu.edu.my

H. Salleh
Department of Mechanical Engineering,
Universiti Tenaga Nasional, Kajang, Malaysia
e-mail: HANIM@uniten.edu.my

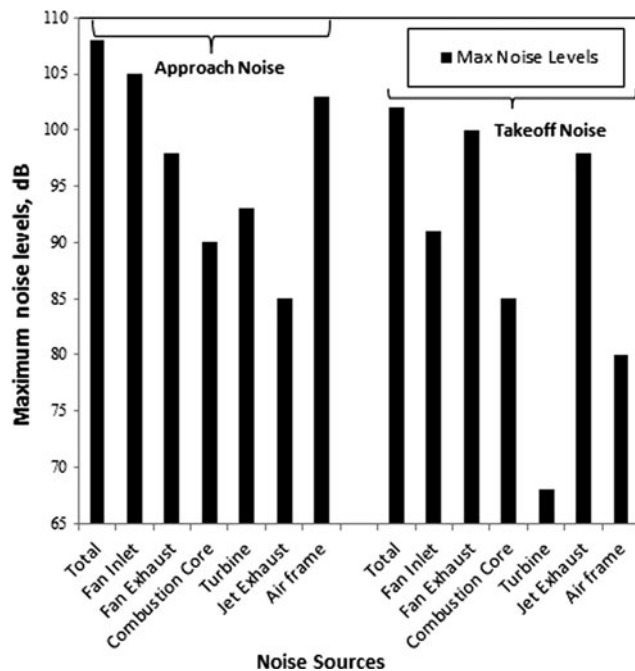


Fig. 1 Graph noise sources versus maximum noise levels in dB

microelectromechanical system (MEMS) fabrication processes (Kim et al. 2009). Fabricated MEMS cantilever generators have been reported to produce output in the μW when harvesting mechanical vibrations in the kHz range. Piezoelectric micro-generators are the perfect candidate to replace batteries as they are easily fabricated, are silicon compatible and demonstrate high efficiencies for mechanical to electrical energy conversion (Horowitz et al. 2005).

One of the niche applications is aero acoustics, where wasted, high dB, high frequency sound generated by aircrafts can be transformed into useful energy. The sound generated by the unsteady aerodynamic forces on propellers is categorized in the domain of aero acoustic. Noise generated during take-off and approaches to landing are the main noise contributions that determining the airport noise levels (Sheplak et al. 1999). Generally, the aircraft engines have noise generated from its engine outlet, slat noise, landing gear, nose wheel, fan exhaust, turbine, fan inlet and jet exhaust. The Aircraft Aerodynamics and Design Group at Stanford University (1999) has the details of aircraft noise is in the range of high dB noise level of 60–110 dB as shown in Fig. 1.

Noise pollution is of increasing community concern and is especially dominant during aircraft landing and take-off.

Exposure to such high dB noise can negatively impact human health since it increases the risk of cardiovascular diseases; causes sleep disturbance and psychological effects. There is a need for miniature acoustic sensors for noise detection system which monitors these hazardous levels of noise.

Aircraft noise monitoring systems deployed on wireless sensor networks can be utilized to trigger alarms when the noise quality level is above the safety standards. The self-sustained wireless sensor network is powered by acoustic energy harvester which is driven by aircraft noise vibration. These acoustic energy harvesters that convert acoustic vibrations into electrical power can be fabricated using microelectromechanical system (MEMS) technology. Such implementation techniques shrink the size of the wireless sensor nodes, leading to a reduction in unit cost for large volumes.

The range of frequency applied from the ambient acoustic as shown in Fig. 2. Horowitz 2005 designed a 50 kHz micro machined piezoelectric diaphragm microphone with a circular piezoelectric ring. The diaphragm transduces acoustical pressure into mechanical deformation, while the piezoelectric material transduces that mechanical deformation into electrical signal (charge or voltage).

This paper details the design of a piezoelectric cantilever beam micro generator for acoustic energy harvesting application. The rest of the paper is organized as follows. Section 2 explains the theoretical design of the piezoelectric working principle and piezoelectric material selection. Section 3 presents the simulation modelling of piezoelectric micro generator. Sample preparation, characterization and preliminary experimental setup and results are presented in Sect. 4. Finally the conclusion is given in Sect. 5.

2 Theoretical design of the piezoelectric micro generator

2.1 Piezoelectric working principle

Piezoelectricity is an electromechanical phenomenon exhibited by a certain solid state materials that converts mechanical energy into electrical energy and vice versa. Electric polarization is developed when there is an applied mechanical stress or strain. Such phenomenon is known as direct piezoelectric effect. Conversely, the reverse

Fig. 2 Frequency range for acoustic devices



piezoelectric effect describes the production of stress and/or strain when an electric field is applied (Horowitz et al. 2005).

A piezoelectric micro generator demonstrates the direct piezoelectric effect where acoustic energy or mechanical vibrations are converted into electrical energy. It has been reported that the cantilever structure with proof mass at the end is the most promising structure for the energy conversion (Roundy et al. 2005). The piezoelectric energy conversion can be described using the equivalent linear spring mass system as shown in Fig. 3 where $z = x - y$ is the net displacement of the mass, M is the lumped mass, K is the spring constant and C is the damping coefficient (Kim et al. 2009).

$$M\ddot{z} + C\dot{z} + Kz = -M\ddot{y} \tag{1}$$

A simplified model of piezoelectricity involves the concept of anions and cations moving in opposite direction under the influence of an electric field or mechanical force (Johnson 2005). The ion charges are neutralized and balanced in the unstrained piezoelectric crystal. When the cantilever is excited due to ambient vibration, the piezoelectric layer deforms and mechanical stress is applied to the cantilever beam. The stress induced in the beam will strain the piezoelectric crystal and generate surface charges due to unbalanced ions. The charges generated on the surface of the piezoelectric crystal are proportional to the potential difference which is a function of the changing stress (Johnson 2005). The charge is measured through the electrodes on top and bottom of the piezoelectric layer which is then converted to AC voltage (Pan et al. 2010)

If we assume that the micro generator operates at resonance frequency, the resonant frequency of spring mass system, ω_n is shown in Eq. 2 where M_{eq} is the equivalent mass and K_{eq} is the equivalent stiffness. At resonance frequency, the cantilever vibrates with maximum deflection. Consequently, maximum charges and potential difference will be produced at the resonance frequency.

$$\omega_n = \sqrt{\frac{K_{eq}}{M_{eq}}} \tag{2}$$

The equivalent stiffness for the cantilever beam can be calculated as shown in Eq. 3 where E is Young modulus

(GPa), I is the moment of inertia, and L is the length of the beam.

$$K_{eq} = \frac{3EI}{L^3} \tag{3}$$

The moment of inertia of the rectangular cantilever beam can be written as shown in Eq. 4 where B_{beam} is the width of the beam and H_{beam} is the height of the cantilever beam.

$$I = \frac{1}{12} B_{beam} * H_{beam}^3 \tag{4}$$

The equivalent mass, m_{eq} for the cantilever beam without any proof mass and with proof mass are given in Eqs. 5, 6 and 7 where ρ is density of the material, W_{beam} is the width of the cantilever beam, H_{beam} is the height of the cantilever beam, L_{beam} is the length of the cantilever beam, M_m is the mass of the proof mass at the end of the cantilever beam and M_{beam} is the mass of the cantilever beam.

$$m_{eq} = \frac{1}{3} \rho * W_{beam} * H_{beam} * L_{beam} \tag{5}$$

$$m_{eq} = M_m + \frac{33}{140} M_{beam} \tag{6}$$

$$M_{beam} = \rho * W_{beam} * H_{beam} * L_{beam} \tag{7}$$

At resonance frequency, the output power is shown in Eq. 8 where P is output power, m is equivalent mass, k is the equivalent stiffness, R is the load resistance, C_b is the capacitance of piezoelectric bimorph, k_{31} is the piezoelectric coupling coefficient, t_c is the thickness of the piezoelectric material, C_p is the elastic constant of the piezoelectric, ϵ is the dielectric constant of the piezoelectric material, A_{in} is the acceleration and ζ is the dimensionless damping ratio which represents the viscous loss from the system. Only the first mode of resonance frequency is considered since it provides the maximum displacement and consequently the maximum output power (Roundy et al. 2005).

$$P = \frac{m^2}{2k} * \frac{RC_b^2 \left[\frac{2k_{31}t_c}{k_2} \right]^2 \frac{C_p A_{in}^2}{\epsilon}}{(4\zeta^2 + k_{31}^4)(RC_b)^2 k + 4\zeta^2 k_{31}^2 RC_b \sqrt{km} + 4\zeta^2 m} \tag{8}$$

Fig. 3 a Schematic representation of the cantilever beam at one fix end b first order model of a resonant system



Table 1 Comparison of piezoelectric thin film materials for energy harvesting application

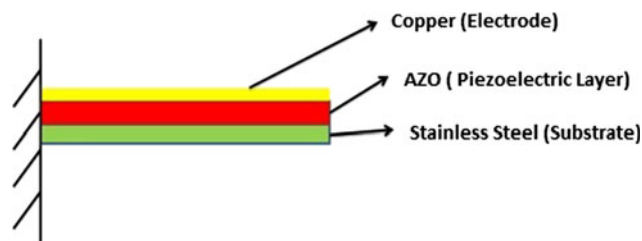
Material	Thin films	Strain coefficient, d_{33} (pm/v)	Coupling coefficient, k	Relative dielectric constant, ϵ	Young modulus, E (GPa)	Density, ρ (g/m ³)
PZT	Lead zirconate titanate	290	0.35	1,700	96	7.70
ZnO	Zinc oxide	12	0.33	10.9	210	5.60
AlN	Aluminium nitride	3.4	0.24	10.5	330	3.26

2.2 Piezoelectric thin film as the material selection

Suitable piezoelectric material is characterized by the product of piezoelectric energy constant (g) and piezoelectric strain coefficient (d) given as $|d \cdot g|$ (Kim et al. 2009). Piezoelectric material can be divided into five types, polycrystalline ceramics, single crystal materials, polymers and thin films (Hyunuk Kim et al. 2009). Piezoelectric thin films offer significant advantages such as generation of large motions, low hysteresis, high sensitivity with wide dynamic ranges and low power requirements (Trolier-Mckinsty and Muralt 2004). The parameters of interest for piezoelectric thin films are piezoelectric strain coefficient, coupling coefficient and relative dielectric constant. The most important parameter is coupling coefficient which describes the effectiveness of energy transformation from electrical to mechanical energy.

The choice of the piezoelectric thin film material also depends on deposition methods, process complexity and CMOS compatibility. Common piezoelectric thin films are zinc oxide (ZnO), aluminium nitride (AlN), and lead zirconate titanate (PZT) (Horowitz 2005). Table 1 shows that PZT provides highest coupling and strain coefficient compared to ZnO and AlN thin films. However, PZT deposition is hazardous due to lead contamination. AlN and ZnO requires relatively low deposition temperature, has high piezoelectric coupling coefficient and excellent bonding to substrate materials such as silicon (Nordin 2008).

ZnO has become a material choice for piezoelectric energy harvesting due to highly resistive c -axis oriented ZnO films. Doping was found to give pronounced effect on both microstructure and piezoelectric properties of ZnO by increasing the longitudinal piezoelectric coefficient (d_{33}) (Bdikin et al. 2010). Many researchers have worked on doping ZnO n-type using group III elements like aluminium (Al), gallium (Ga) and indium (In) (Hamid 2009). This process was found to produce ZnO films with more n-type conductivity, improving its transparency and conductivity. Doping of ZnO had improved not only the electrical properties of the film but also its thermal stability. Aluminium is found to be the best dopant as it produces films with the highest conductivity and transparency as compared to any other dopant (Hamid 2009). Therefore,

**Fig. 4** Piezoelectric cantilever beam design

aluminium doped zinc oxide (AZO) was chosen as the piezoelectric material for this work.

3 Simulation modeling of piezoelectric micro generator

The prototype cantilever structure consists of three layers namely: stainless Steel, AZO, and copper electrode as shown in Fig. 4. The substrate is stainless steel and the chosen piezoelectric layer is AZO. The copper was deposited on top of the piezoelectric layer. The cantilever beam is fixed at one end. The device dimensions are shown in Table 2.

3.1 Material properties

The three material properties matrix that are crucial for analysis of piezoelectric thin films are stress coefficient (d^t), dielectric constant (ϵ), and stiffness matrix (C), are shown in Eqs. 9, 10 and 11, respectively. The material properties for each layer of the piezoelectric micro generator are summarized in Table 3.

$$[d]^t = \begin{bmatrix} 0 & 0 & d_{31} \\ 0 & 0 & d_{31} \\ 0 & 0 & d_{33} \\ 0 & 0 & 0 \\ d_{15} & 0 & 0 \\ 0 & -d_{15} & 0 \end{bmatrix} = \begin{bmatrix} 0 & 0 & -5.43e-06 \\ 0 & 0 & -5.43e-06 \\ 0 & 0 & 1.167e-05 \\ 0 & 0 & 0 \\ 1.1344e-05 & 0 & 0 \\ 0 & -1.1344e-05 & 0 \end{bmatrix} \text{ C/m}^2 \quad (9)$$

Table 2 Device dimension

Material	Length (μm)	Width (μm)	Thickness (μm)
Stainless steel	20,000	20,000	16.8
Aluminium doped zinc oxide (AZO)	20,000	20,000	36.8
Copper	20,000	20,000	5

Table 3 Material properties

Material used in experiment	Material used for simulation	Poisson ratio, ν	Young modulus, E (Pa)	Density, ρ (kg/m ³)	Thermal conductivity W/m-K (at 100°C)	Electrical conductivity (Sm ⁻¹)
Stainless steel	Fe	0.305	240×10^9	8,000	16.2	0.862×10^6
Aluminium doped zinc oxide	Zinc oxide	–	[C] _{6×6}	5,610	–	–
Copper	Cu	0.326	1.19×10^9	8,940	401	59.6×10^6

While, the piezoelectric zinc oxide dielectric constant in matrix form is in Eq. 10.

$$[\varepsilon] = \begin{bmatrix} 8.55 & 0 & 0 \\ 0 & 8.55 & 0 \\ 0 & 0 & 10.2 \end{bmatrix} \quad (10)$$

Piezoelectric zinc oxide stiffness matrix (Young modulus) is shown in Eq. 11.

$$[C] = \begin{bmatrix} 20.97 & 12.11 & 10.51 & 0 & 0 & 0 \\ 12.11 & 20.97 & 10.51 & 0 & 0 & 0 \\ 10.51 & 10.51 & 21.09 & 0 & 0 & 0 \\ 0 & 0 & 0 & 4.43 & 0 & 0 \\ 0 & 0 & 0 & 0 & 4.24 & 0 \\ 0 & 0 & 0 & 0 & 0 & 4.24 \end{bmatrix} \quad (11)$$

* $10^{10} N/m^2$

The 3D view and fabrication steps are shown in Fig. 5 and Table 4, respectively. Stainless steel acts as the substrate to control the bow of the structure. AZO was chosen as the piezoelectric layer with thickness of 36.4 μm. Copper electrode was deposited on top of the piezoelectric layer. The size of the cantilever is 20,000 μm × 20,000 μm with thickness of 58.6 μm.

3.2 Finite element analysis

The device was modelled and simulated using a finite element (FEM) simulator, CoventorWare[®] which has the capabilities of producing a 3D model based on the layout and the fabrication process. Finite element modelling analysis was used to predict the resonance frequency of the maximum displacement of vibration which therefore provides maximum output power for piezoelectric micro generator (Ralib et al. 2010). The applied boundary condition is at the fixed end of the cantilever beam and

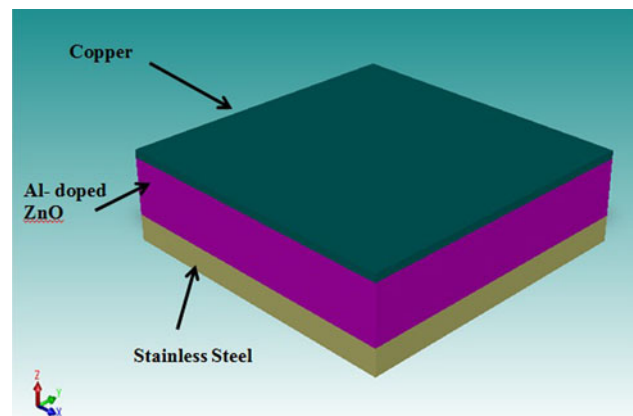


Fig. 5 3D view of piezoelectric cantilever beam design

pressure is applied at the bottom of the piezoelectric layer as shown in Table 5. Once the model specifications have been completed, it was meshed using Manhattan Bricks, which are preferred for rectangular structures. The mesh details are summarized in Table 6.

3.3 Simulation result and discussion

MemMech piezoelectric modal analysis was done to compute the resonance modes of the structure. Simulation result shows that the highest displacement is at the z direction as shown in Fig. 6. Fifty modes were simulated, where the mode with the highest displacement was identified as the mode of interest. Figure 7 displays various vibration mode of piezoelectric energy harvester. Mode 48 of 32.8 kHz is of the most interest. The following harmonic analysis will be based on this frequency.

Harmonic analysis computes a displacement solution based on a user range of input harmonic frequencies to find the best resonance frequency which has maximum displacement (Ralib et al. 2010). A total of 50 frequencies at the

Table 4 Fabrication steps in simulation

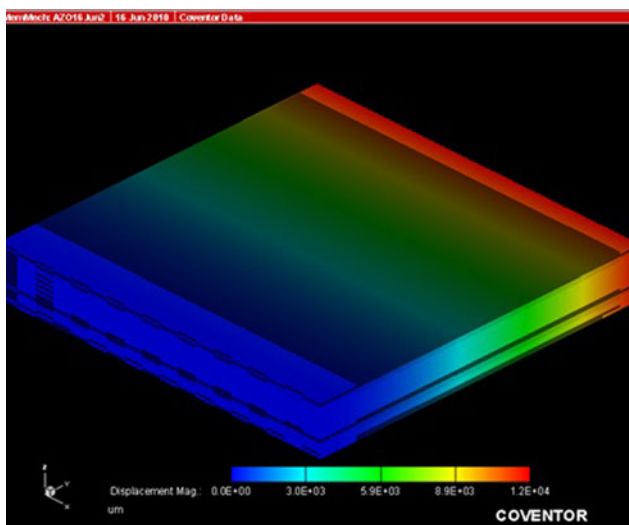
No.	Step name	Action	Layer name	Material name	Thickness (μm)	Mask name
0	Substrate	Substrate	Substrate	Stainless steel	16.8	Substrate mask
1	Stack material	Stack material	Piezoelectric	ZnO	36.4	
2	Stack material	Stack material	Electrode	Copper	5	

Table 5 Surface boundary condition

Layer	Surface boundary condition
Stainless steel	Left edge fixed
Zinc oxide	Left edge fixed
Zinc oxide	Pzt_bot (0.0005 Pa)

Table 6 Meshing properties

Nu.	Layer name	Material name	Thickness (μm)	Meshing types	Element size (X, Y, Z)	Aspect ratio
0	Substrate	Stainless steel	16.8	Manhattan bricks	(1,000, 1,000, 20)	43
1	Piezoelectric	ZnO	36.4	Manhattan bricks	(1,000, 1,000, 20)	43
2	Electrode	Copper	5	Manhattan bricks	(1,000, 1,000, 5)	43

**Fig. 6** MemMech piezoelectric analysis

range of 32.3111–34.4667 kHz were simulated. Simulation results shows that maximum z axis deflection of 1.735 μm was found at the resonance frequency of 32.92 kHz. Figure 8 shows the graph of displacement versus frequency generated. The graph shows expected sharp change in the displacement at z direction as the frequency reached 32.92 kHz.

4 Fabrication of piezoelectric micro generator

Figure 9 shows the process flow for sample preparation steps of piezoelectric micro generator. The stainless steel was

chosen as the substrate. AZO was sputtered using ULVAC sputtering machine. Copper material was pasted on top of the AZO as the electrode using carbon paste. The sample was characterized by X-ray diffraction to evaluate the orientation and crystallization qualities. The scanning electron microscopy (SEM) was used to measure the thickness of the sample and evaluate its surface morphology.

4.1 Aluminium doped zinc oxide (AZO) RF magnetron sputtering

Piezoelectric deposition techniques consist of various method and techniques such as sputtering methods, chemical vapor deposition (CVD) techniques, and spin on sol–gel processing. Highly oriented AZO were prepared by RF Magnetron sputtering on stainless steel substrate. The optimized parameters for RF magnetron sputtering are summarized in Table 7. Six samples with same parameters were prepared as shown in Fig. 10.

4.2 Sample characterization result

4.2.1 Crystalline structure

Good piezoelectric ZnO thin films are expected to show c -axis orientation in 002 direction, band gap of 3.37 eV, refractive index 2.008 and high transparency in the visible region (Gokhale et al. 2008). X Ray diffraction was performed on the samples and its intensity versus 2 theta. X Ray diffraction confirms that the thin films has a

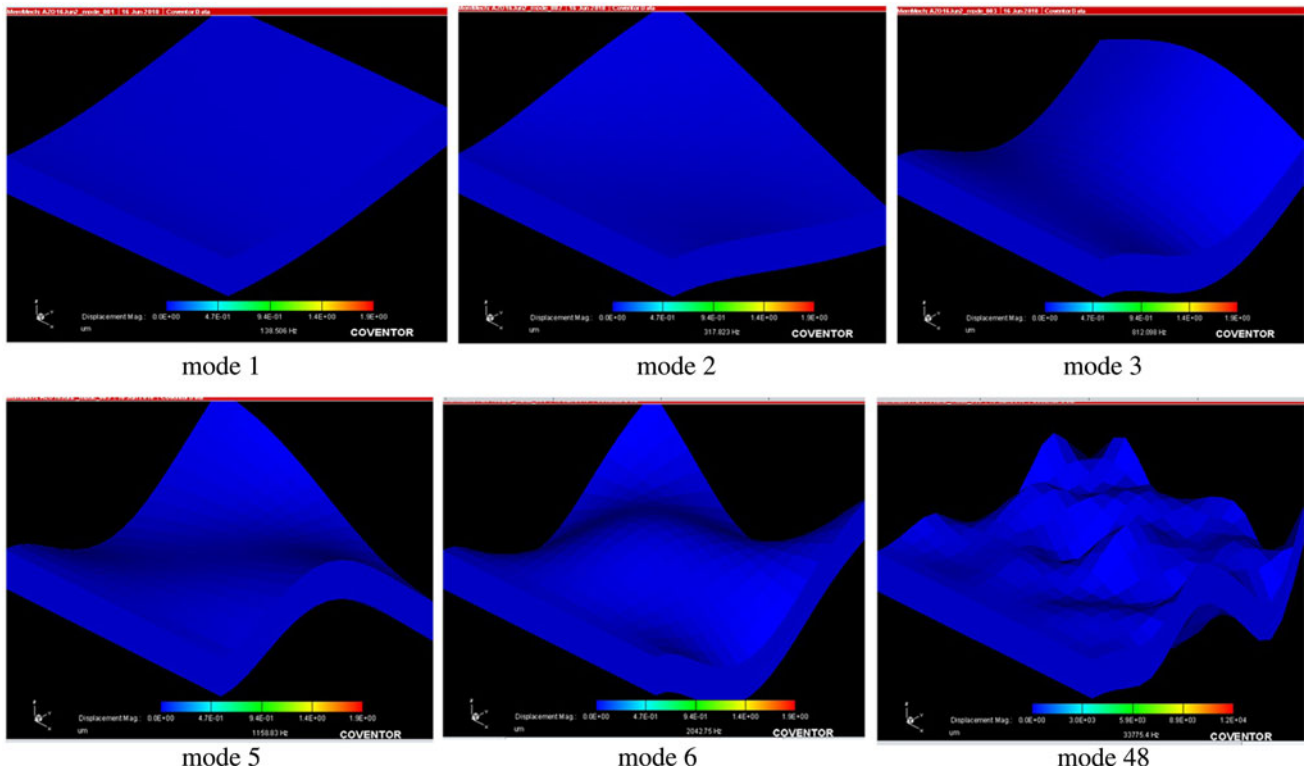
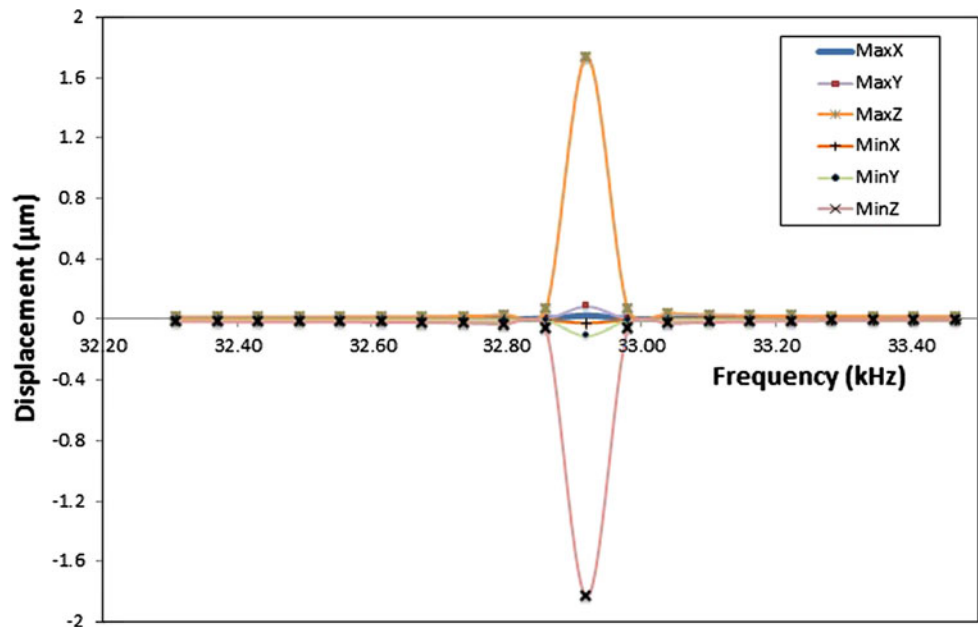


Fig. 7 MemMech modal analysis

Fig. 8 Piezoelectric harmonic analysis displacement versus frequency

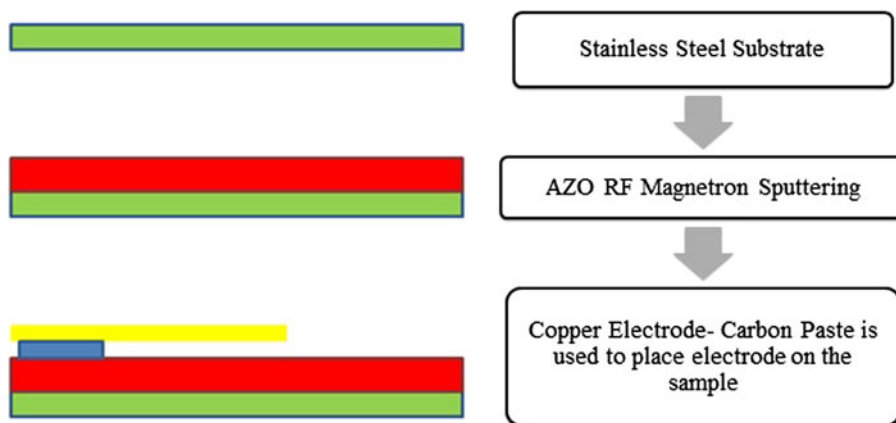


preferred orientation with *c*-axis perpendicular to substrate (Trolrier-Mckinstry and Muralt 2004). The *c*-axis orientation at 002 peak was clearly shown at 2 theta values of 34.4° which is very close with pure ZnO crystal orientation (34.45°) as shown in Fig. 11. The diffraction angle of 002 plane of AZO thin film was shifted towards lower angle and smaller to standard ZnO crystal due to ionization of

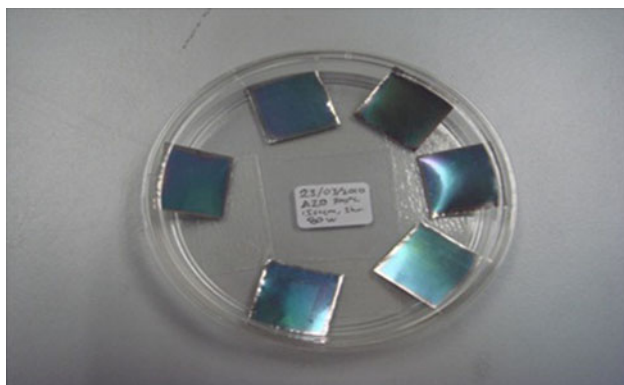
ZnO rather than Al doping. (Jeong et al. 2003). The intensity of AZO at 2 theta of 34.4° is 2,108.

4.2.2 Surface morphology

The surface morphology of the AZO thin film structure was examined using scanning electron microscopy at 500×

Fig. 9 Fabrication steps for sample preparation**Table 7** RF magnetron sputtering parameters

Parameter	Value
Sputtering gas	Argon
Working pressure	5 mTorr
Target	AZO
Substrate material	Stainless steel
Substrate temperature	300°C
RF power	80 W
Deposition time	1 h
Thickness	38.4 μm

**Fig. 10** Sample of aluminium doped zinc oxide sputtered on stainless steel

magnification and is shown in Fig. 12a. The thickness was measured through the cross section of the sample as shown in Fig. 12b. The thickness of AZO thin film is 38.4 μm and the thickness of stainless steel is 16 μm .

4.3 Experimental setup and results

The measurement system was schematically shown in Fig. 13. The sample was placed on the ultrasonic cleaner that act as the vibration shaker. The frequency of the

vibration from the ultrasonic cleaner is 30 kHz and the power is 80 W. The generated voltage was measured using digital multimeter UT803.

4.3.1 Experimental result and discussion

Figure 14 shows the open circuit voltage versus time, RMS output voltage versus time and calculated RMS output power at load resistance of 1 k Ω versus time, respectively. The result in Table 8 shows that the maximum output of open circuit voltage produced is approximately 345.4 mV. The closed circuit voltage (CCV) is measured as a function of load resistance and the input frequency of 30 kHz. The output power is calculated by assuming the load resistance is 1 k Ω . The calculated peak power is calculated with load resistance of 1 k Ω is approximately 59.63 μW . This measured power level is satisfactory to power a miniature wireless acoustic sensor nodes for high dB noise detection monitoring system generated by aircrafts.

5 Conclusion

Piezoelectric vibration energy harvester is a very attractive method to power wireless sensor networks due to their higher power density, robustness and simplicity. This paper presents the simulation and experimental study of a piezoelectric micro generator for aero acoustic application. Aluminium doped zinc oxide was chosen as the piezoelectric material due to its excellence bonding properties to substrate material and high piezoelectric coupling coefficient. Finite element simulation analysis was done to simulate the resonance frequency which provides maximum displacement of vibration and maximum output power. For sample preparation, aluminium doped zinc oxide piezoelectric thin film was RF-sputtered on stainless

Fig. 11 X-Ray diffraction result intensity versus 2theta

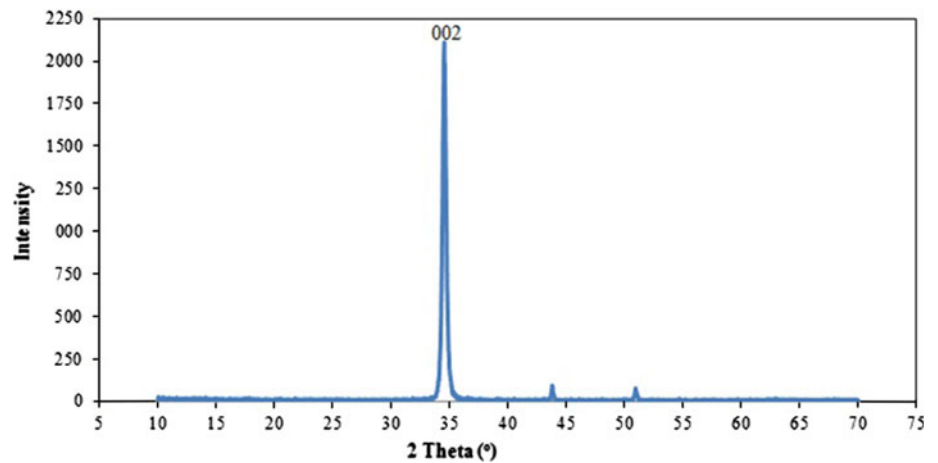


Fig. 12 **a** Surface morphology at ×500 magnifications. **b** Cross-section thickness of the sample

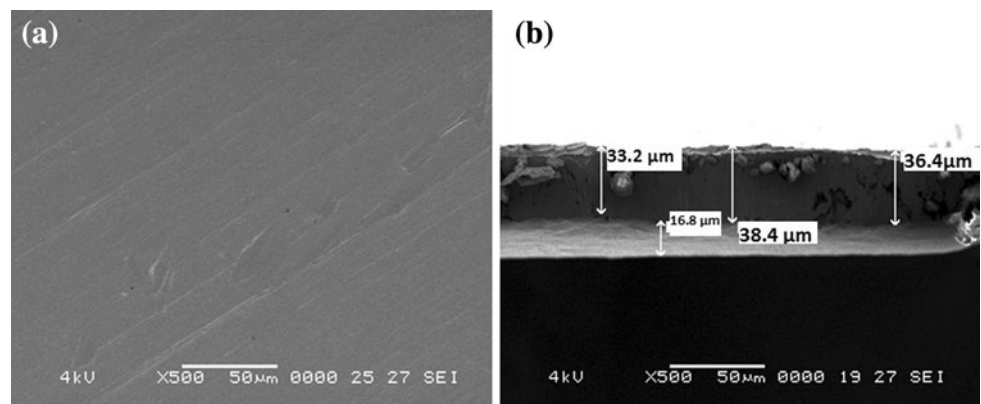
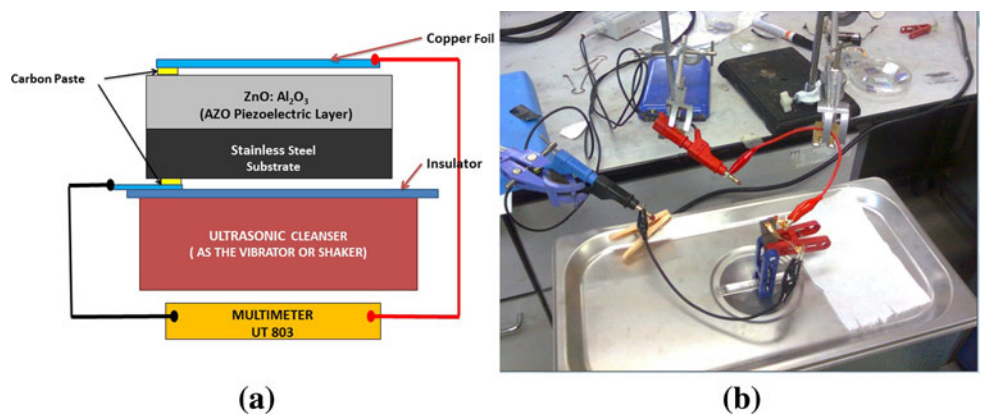


Fig. 13 **a** Schematic illustration of voltage generation of piezoelectric micro generator. **b** Preliminary experiment setup for piezoelectric micro generator



steel substrate thin film. Characterization was performed using X-ray diffraction (XRD) and scanning electron microscopy (SEM) to evaluate the piezoelectric qualities and surface morphology, respectively. The *c*-axis orientation at 002 peak was clearly shown at 2 theta values of 34.4° which is very close with pure ZnO crystal orientation. Experimental measurements indicate that

approximately 345.4 mV AC output voltage (open circuit voltage) is produced at vibration frequencies of 30 kHz. This is in accordance with the Coventorware™ simulation result that shows resonance frequency of 32.92 kHz. This measured power level is sufficient to power a miniature wireless acoustic sensor nodes for high dB aircraft noise detection monitoring.

Fig. 14 **a** Open circuit voltage versus time, **b** RMS Output Voltage versus time, **c** calculated output power at load resistance of 1 k Ω versus time

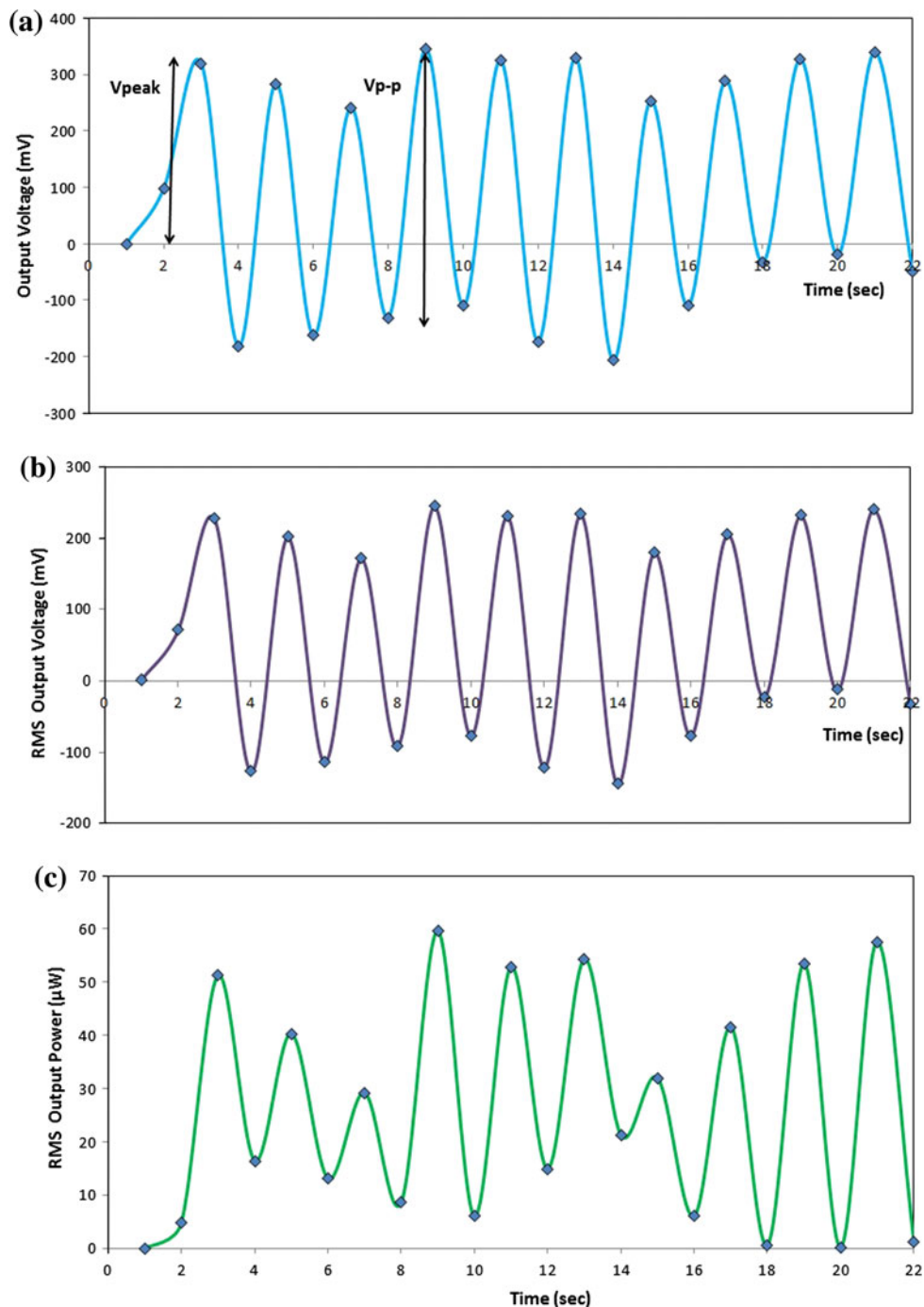


Table 8 Peak voltage and peak power for experiment

Frequency (kHz)	30
Maximum open circuit voltage, OCV (mV)	345.4
Maximum RMS output voltage (mV)	244.20
Calculated peak power at load resistance of 1 k Ω (μ W)	59.63

Acknowledgments The research was collaboration between Universiti Tenaga Nasional and International Islamic University Malaysia. The piezoelectric energy harvester was fabricated at International

Islamic University Malaysia. The authors would like to thank Husni Kamal Bin Mohd. Said for his expertise and assistance during the sputtering process. All authors are also grateful for the support and funding from Tenaga Nasional Berhad Malaysia

References

- Bdikin IK, Gracio J, Ayouchi R, Schwarz R, Kholkin AL (2010) Local piezoelectric properties of ZnO thin films prepared by RF-plasma-assisted pulsed-laser deposition method. *Nanotechnology*, vol 21, No. 23

- Choi WJ, Jeon Y, Jeong J-H, Sood R, Kim SG (2006) Energy harvesting MEMS device based on thin film piezoelectric cantilevers. *Electroceramics* 17:2–4
- Gokhale N, Parmar M, Rajanna K, Nayak MM (2008) Piezoelectric zinc oxide thin film for MEMS application: a comparative study. 3rd international conference on sensing technology, 30 Nov–3 Dec
- Hamid HBA (2009) Fabrication, structural and electrical characteristics of zinc oxide thin films by direct current sputtering
- Horowitz SB (2005) Development of MEMS based acoustic energy harvester
- Horowitz SB, Nishida T, Cattafesta LN, Sheplak M (2005) Design and characterization of a micromachined piezoelectric microphone, 26th AIAA aeroacoustics conference, 23–25 May 2005
- Jeong SH, Lee JW, Lee SB, Boo JH (2003) Deposition of aluminium doped zinc oxide films by RF magnetron sputtering and study of their structural, electrical and optical properties. *Thin Solid Films* 435(1–2):78–82
- Johnson RL (2005) Characterization of piezoelectric ZnO thin films and the fabrication of piezoelectric micro-cantilevers, pp 8–9
- Kim H, Tadesse Y, Priya S, Inman DJ (2009) *Energy harvesting technologies* (e-book). Springerlink
- Kok SL, White NM, Harris NR (2008) A free standing thick film piezoelectric energy harvester IEEE sensors 2008 conference
- Liu J-Q, Fang H-B, Xu Z-Y, Mao X-H, Shen X-C, Chen D, Liao H, Cai B-C (2008) A MEMS-based piezoelectric power generator array for vibration energy harvesting. *Microelectron J* 39:802–806
- Nordin AN (2008) Design, implementation and characterization of temperature compensated SAW resonators in CMOS Technology for RF Oscillators
- Pan CT, Liu ZH, Chen YC, Liu CF (2010) Design and fabrication of flexible piezo-microgenerator by depositing ZnO thin films on PET substrates. *Sens Actuat A Phys* 159:96–104
- Paradiso JA, Starner T (2005) Energy scavenging for mobile and wireless electronics. *Pervasive computing*. IEEE CS IEEE ComSoc 4(1):18–27
- Ralib AAM, Nurashikin A, Salleh H (2010) Simulation of MEMS piezoelectric energy harvester, DTIP. Symposium on design, test, integration and packaging of MEMS/MOEMS, 5–7 May 2010
- Roundy S, Leland ES, Baker J, Carleton E, Reilly E, Lai E, Otis B, Rabaey JM, Wright PK, Sundararajan V (2005) Improving power output for vibration-based energy scavengers, pervasive computing
- Sheplak M, Seiner JM, Breuer KS, Schmidt MA (1999) A MEMS microphone for aeroacoustics measurements, AIAA 99-0606, Reno, NV, January 1999
- The Aircraft Aerodynamics and Design Group at Stanford University (1999) The Aircraft Aerodynamics and Design Group at Stanford University viewed 20 May 2010 (online). Available from <http://adg.stanford.edu/aa241>
- Trolier-Mckinstry S, Muralt P (2004) Thin film piezoelectric for MEMS. *Electroceramics* 12:7–17